Available online at www.sciencedirect.com
ScienceDirect
Polymer 49 (2008) 1567–1578
polymer
www.elsevier.com/locate/polymer

Comparison of thermomechanical properties of statistical, gradient and block copolymers of isobornyl acrylate and *n*-butyl acrylate with various acrylate homopolymers

Wojciech Jakubowski [a], Azhar Juhari [b], Andreas Best [b], Kaloian Koynov [b], Tadeusz Pakula [b,1], Krzysztof Matyjaszewski [a,*]

[a] *Center for Macromolecular Engineering, Department of Chemistry, Carnegie Mellon University, 4400 Fifth Avenue, Pittsburgh, PA 15213, USA*
[b] *Max-Planck-Institute for Polymer Research, Ackermannweg 10, 55128 Mainz, Germany*

Received 12 December 2007; received in revised form 12 January 2008; accepted 17 January 2008
Available online 29 January 2008

Abstract

Well-defined statistical, gradient and block copolymers consisting of isobornyl acrylate (IBA) and *n*-butyl acrylate (*n*BA) were synthesized via atom transfer radical polymerization (ATRP). To investigate structure–property correlation, copolymers were prepared with systematically varied molecular weights and compositions. Thermomechanical properties of synthesized materials were analyzed via differential scanning calorimetry (DSC), dynamic mechanical analyses (DMA) and small-angle X-ray scattering (SAXS). Glass transition temperature (T_g) of the resulting statistical poly(isobornyl acrylate-*co*-*n*-butyl acrylate) (P(IBA-*co*-*n*BA)) copolymers was tuned by changing the monomer feed. This way, it was possible to generate materials which can mimic thermal behavior of several homopolymers, such as poly(*t*-butyl acrylate) (P*t*BA), poly(methyl acrylate) (PMA), poly(ethyl acrylate) (PEA) and poly(*n*-propyl acrylate) (PPA). Although statistical copolymers had the same thermal properties as their homopolymer equivalents, DMA measurements revealed that they are much softer materials. While statistical copolymers showed a single T_g, block copolymers showed two T_gs and DSC thermogram for the gradient copolymer indicated a single, but very broad, glass transition. The mechanical properties of block and gradient copolymers were compared to the statistical copolymers with the same IBA/*n*BA composition.

Keywords: Atom transfer radical polymerization (ATRP); Block copolymer; Gradient copolymer

1. Introduction

The constantly advancing technologies demand new, high performance and more specialized materials with highly specialized functions [1–9]. Such materials are no longer one (monolithic) component systems. Thus, the investigation on systems built with two or more components is in demand, especially for structure–property correlations. One example of a two-component system is block copolymer, in which the instantaneous composition changes discontinuously and abruptly along the chain. Another example is a gradient copolymer, in which instantaneous composition varies continuously along the chain contour. Both these copolymers are synthesized by controlled/living polymerization techniques [10]. In contrast to block and gradient copolymers, statistical copolymer composition is constant along the polymer chain. These three copolymers, even if built with the same type and number of units, may have completely different properties.

Controlled/living radical polymerization (CRP) technology was developed in mid 1990s and can be applied to the preparation of many different (co)polymers [11,12]. These CRP processes, such us atom transfer radical polymerization (ATRP) [13–15], nitroxide mediated polymerization (NMP) [16,17], or reversible addition–fragmentation chain transfer (RAFT) [18] can be conducted at convenient temperatures,

* Corresponding author. Tel.: +1 412 268 3209; fax: +1 412 268 6897.
E-mail address: km3b@andrew.cmu.edu (K. Matyjaszewski).
[1] Deceased on 06.07.2005.

0032-3861/$ - see front matter © 2008 Elsevier Ltd. All rights reserved.
doi:10.1016/j.polymer.2008.01.047

does not require extensive purification of the monomers or solvents and can be conducted in bulk, solution, aqueous suspension, emulsion, etc [19]. These techniques allow the preparation of polymers with predetermined molecular weights, low polydispersity and controlled functionality, composition and topology. Because radical polymerization is very tolerant of functional groups, a broad range of unsaturated molecules can be polymerized [20]. This provides an opportunity to form well-defined block, gradient and statistical copolymers with a wide-ranging spectrum of properties [10g,21]. The general mechanism of ATRP, as well as other CRP techniques, relies on creating a dynamic equilibrium between a low concentration of active propagating chains and a large amount of dormant chains, which are unable to propagate or self-terminate (Fig. 1) [22–24]. Thus, the probability of bimolecular termination reactions is decreased and the radical polymerization behaves as a living system and, as a result, many different (co)polymers may be precisely constructed. ATRP was already used for preparation of many different block, gradient and statistical copolymers [25–27]. Their thermal and mechanical properties are quite different [28–31].

This article reports on a study of the structure–property correlations of different copolymers built with *n*-butyl acrylate (*n*BA) and isobornyl acrylate (IBA). The primary goal of this work was to compare thermomechanical properties of block, gradient and statistical copolymers of *n*BA and IBA with various acrylate homopolymers (Scheme 1). The choice of *n*BA and IBA was dictated by very different thermal properties of the resulting homopolymers, glass transition temperature (T_g) of P*n*BA is −54 °C when T_g of PIBA is 94 °C [32]. Thus, their copolymerization with carefully selected ratios should result in polymers with thermal properties similar to acrylate homopolymers: poly(*t*-butyl acrylate) (P*t*BA), poly(methyl acrylate) (PMA), poly(ethyl acrylate) (PEA) and poly(*n*-propyl acrylate) (PPA). Although thermal properties of copolymers and homopolymers will be similar, their mechanical properties may significantly differ, depending on type of building units and their arrangement. Presented research may be important since, in a similar way, one can copolymerize other monomers and affect not only physical properties of final polymer materials but also their degradation rates and toxicity, both of which are very important, for example, in biomedical applications.

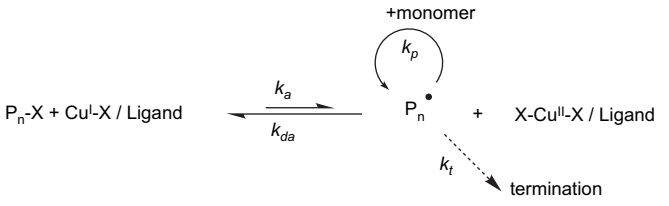

Fig. 1. Mechanism for atom transfer radical polymerization (ATRP) where: P_nX – dormant species, $P_n^\bullet$ – propagating species, Cu^I–X/Ligand – transition metal complex (activator), X–Cu^{II}–X/Ligand – oxidized metal complex (deactivator), k_a – rate constants of activation, k_{da} – rate constant of deactivation, k_p – rate constant of propagation, k_t – rate constant of termination.

2. Experimental part

2.1. Chemicals

Methyl acrylate (MA) (Acros, 99%), ethyl acrylate (EA) (Acros, 99%), *n*-propyl acrylate (PA) (Scientific Polymer Products Inc., 99%), *n*-butyl acrylate (*n*BA) (Acros, 99%), *t*-butyl acrylate (*t*BA) (Acros, 99%) and isobornyl acrylate (IBA) (Aldrich, 99%) were dried over calcium hydrate and distilled under reduced pressure. Ethyl 2-bromoisobutyrate (EtBrIB) (Acros, 98%), copper(II) bromide (Acros, 99%), *N*,*N*,*N*′,*N*″,*N*″-pentamethyldiethylenetriamine (PMDETA) (Aldrich, 99%), anisole (Aldrich, 99%), acetone (Acros, 98%), diphenyl ether (DPE) (Acros, 99%) were used as received. Copper(I) bromide (Acros, 95%) was washed with glacial acetic acid in order to remove any soluble oxidized species, filtered, washed with ethanol and dried.

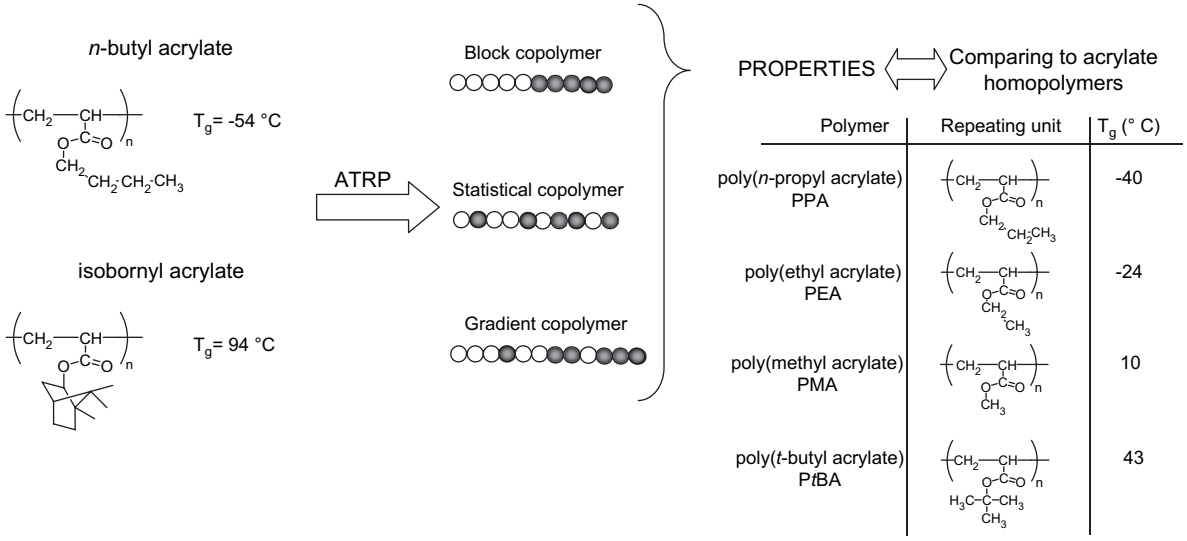

Scheme 1. Copolymerization of isobornyl acrylate and *n*-butyl acrylate in different fashion and comparison of properties of resulting copolymers with acrylate based homopolymers such as P*t*BA, PMA, PEA and PPA.

2.2. General procedure for the preparation of homopolymers using ATRP

CuBr (7.1 mg, 4.9×10^{-2} mmol) was placed in a 10 ml Schlenk flask, and the flask was thoroughly purged by vacuum and flushed with nitrogen. Nitrogen-purged *n*BA (3.5 ml, 24 mmol) was added via syringe. A solution of PMDETA (8.8 μl, 4.2×10^{-2} mmol) in degassed acetone (0.5 ml) was added, and the mixture was stirred for 15 min in order to preform the CuBr/PMDETA complex [33]. Next, EtBrIB initiator (7.2 μl, 4.9×10^{-2} mmol) in purged anisole (0.3 ml) was added. The flask was then transferred to a thermostated oil bath at 50 °C, and the initial kinetic sample was taken. The polymerization was stopped ($M_{n,\ GPC} = 47\,900$, $M_w/M_n = 1.07$, $M_{n,\ theor} = 40\,800$) by opening the flask and exposing the catalyst to air.

The same procedure was used for the polymerization of other monomers: MA, EA, PA, *t*BA and IBA.

2.3. General procedure for the preparation of statistical copolymer poly(isobornyl acrylate-co-n-butyl acrylate), P(IBA-co-nBA), using ATRP

CuBr (5.7 mg, 4.0×10^{-2} mmol) was placed in a 10 ml Schlenk flask, and the flask was thoroughly purged by vacuum and flushed with nitrogen. Nitrogen-purged *n*BA (2.8 ml, 19 mmol) and IBA (2.5 ml, 12 mmol) were added via syringe. A solution of PMDETA (10 μl, 3.6×10^{-2} mmol) in degassed acetone (1.0 ml) was added, and the mixture was stirred for 15 min in order to preform the CuBr/PMDETA complex. Next, EtBrIB initiator (25 μl, 3.3×10^{-2} mmol) in purged anisole (0.3 ml) was added. The flask was then transferred to a thermostated oil bath at 50 °C, and the initial kinetic sample was taken. The polymerization was stopped ($M_{n,\ GPC} = 69\,000$, $M_w/M_n = 1.06$, $M_{n,\ theor} = 67\,000$) by opening the flask and exposing the catalyst to air.

2.4. Synthesis of diblock copolymer poly(isobornyl acrylate)-b-poly(n-butyl acrylate), PIBA-b-PnBA, using ATRP

PIBA macroinitiator ($M_{n,\ GPC} = 28\,500$, $M_w/M_n = 1.06$) (0.5 g, 1.8×10^{-2} mmol) and CuBr (6.3 mg, 4.4×10^{-2} mol) were placed in a 10 ml Schlenk flask, and the flask was thoroughly purged by vacuum and flushed with nitrogen. Nitrogen-purged *n*BA (1.48 ml, 10 mmol) and anisole (0.3 ml) were added via syringe. A solution of PMDETA (9.7 μl, 3.5×10^{-2} mmol) in degassed acetone was added, and the mixture was stirred for 15 min in order to preform the CuBr/PMDETA complex. The flask was then transferred to a thermostated oil bath at 50 °C, and the initial kinetic sample was taken. The polymerization was stopped ($M_{n,\ GPC} = 54\,600$, $M_w/M_n = 1.12$, $M_{n,\ theor} = 46\,300$) by opening the flask and exposing the catalyst to air.

2.5. Synthesis of gradient copolymer poly(isobornyl acrylate-grad-n-butyl acrylate), P(IBA-grad-nBA), using ATRP

In the primary reaction Schlenk flask, CuBr (29.2 mg, 20.4×10^{-2} mol) and $CuBr_2$ (2.2 mg, 1.5×10^{-2} mol) were placed and the flask was thoroughly purged by vacuum and flushed with nitrogen. Nitrogen-purged *n*BA (4.45 ml, 31.2 mmol) and PMDETA (49 μl, 18×10^{-2} mmol) in anisole (1.0 ml) were added via syringe. Similarly, secondary reaction Schlenk flask was prepared with CuBr (29.2 mg, 20.4×10^{-2} mol), $CuBr_2$ (2.2 mg, 1.5×10^{-2} mol), IBA (4.60 ml, 22.1 mmol), PMDETA (49 μl, 18×10^{-2} mmol) and DPE (1.0 ml). After stirring the mixtures for 10 min, initial samples were taken from both the primary and secondary mixtures. The secondary reaction mixture was transferred into an airtight syringe and assembled to a syringe pump. The primary flask was placed in a preheated oil bath at 70 °C, and then EtBrIB initiator (15 μl, 10×10^{-2} mmol) was added. Simultaneously, the continuous addition of the secondary reaction mixture to the primary one was started at a rate of 0.86 ml/h. Samples were taken every 30 min. After 5.4 h, the IBA addition was complete. The reaction was stopped after 6.3 h by exposing the reaction mixture to air. Monomer conversion was found to be 91% *n*BA and 70% IBA as detected by GC ($M_{n,\ GPC} = 74\,800$, $M_w/M_n = 1.13$, $M_{n,\ theor} = 62\,300$).

2.6. Purification of synthesized polymers

After polymerization was finished, polymer solution was diluted with THF and filtered through alumina column. Next, excess of solvent was removed under reduced pressure and polymer was precipitated in to cold methanol. Precipitation procedure was repeated two times and next polymer was dried under vacuum at 70 °C for 24 h. The purity of polymer materials was confirmed by ^{1}H NMR.

2.7. General analysis

Molecular weight and polydispersity were determined by gel permeation chromatography (GPC), conducted with a Waters 515 pump and Waters 2414 differential refractometer using PSS columns (Styrogel 10^5, 10^3, 10^2 Å) in THF as an eluent at 35 °C and at a flow rate of 1 ml/min. Linear polystyrene standards and poly(methyl methacrylate) were used for calibration. Conversion of monomers were determined using a Shimadzu GC 14-A gas chromatograph (GC) equipped with a FID detector using a J&W Scientific 30 m DB WAX Megabore column with anisole (or DPE) as an internal standard. Conversion was calculated by detecting the decrease of the monomer peak area relative to the peak areas of the standard. ^{1}H NMR spectroscopy was performed using Bruker 300 MHz instrument with $CDCl_3$ as a solvent.

2.7.1. Differential scanning calorimetry (DSC)

Thermal characterization of polymers was performed using a Mettler DSC-30 calorimeter. Experiments were conducted

with cooling and heating rates of 10 K/min. The glass transition temperatures (T_g) were determined from the second heating run at the inflection point.

2.7.2. Dynamic mechanical analyses (DMA)

DMA have been performed using an advanced rheometric expansion system (ARES) equipped with a force-rebalanced transducer. Shear deformation was applied under conditions of controlled deformation amplitude, which was kept in the range of the linear viscoelastic response of studied samples. Plate–plate geometry has been used with plate diameters of 6 mm. The gap between plates (sample thickness) was about 1 mm. Experiments have been performed under a dry nitrogen atmosphere. Frequency dependencies of the storage (G') and the loss (G'') parts of the shear modulus have been determined from frequency sweeps measured within the frequency range 10^{-2}–10^{2} rad/s at various temperatures. Master curves for G' and G'' at a reference temperature have been obtained using the time–temperature superposition, i.e., shifting the data recorded at various temperatures only along the frequency coordinate.

2.7.3. Small-angle X-ray scattering (SAXS) analyses

SAXS measurements were conducted using a rotating anode (Rigaku RA-Micro 7) X-ray beam with a pinhole collimation and a two-dimensional detector (Bruker Highstar) with 1024×1024 pixels. A double graphite monochromator for the Cu Kα radiation ($\lambda = 0.154$ nm) was used. The beam diameter was about 0.8 mm, and the sample to detector distance was 1.8 m. The recorded scattered intensity distributions were integrated over the azimuthal angle and are presented as functions of the scattering vector ($s = 2\sin(\theta)/\lambda$, where 2θ is the scattering angle).

3. Results and discussion

3.1. Synthesis

3.1.1. Synthesis of homopolymers, statistical and block copolymers

Synthesis of homopolymers and various copolymers of *n*BA and IBA was performed under normal ATRP conditions. Homopolymer standards were prepared first: PMA, PEA, P*n*PA PIBA, P*n*BA and P*t*BA. Next, statistical copolymers of *n*BA and IBA with different molecular weights and compositions were synthesized. In all ATRP reactions CuBr/PMDETA complex was used as commercially available and well-known to mediate controlled polymerization of acrylate monomers. Polymerizations were performed at 50 °C in acetone/anisole mixture using EtBrIB as initiator. The list of all prepared materials is shown in Table 1. Scheme 2 presents the range of changed compositional parameters in P(IBA-*co*-*n*BA) copolymers. The red and green lines indicate polymers with similar DP but different IBA/*n*BA ratio for copolymers with high and low molecular weight, respectively. Copolymers with similar IBA/*n*BA ratio but with different degree of polymerization (DP), i.e., the blue line, were also synthesized. This set of materials should scan all structure–property correlation for statistical copolymers.

Next, block copolymer PIBA-*b*-P*n*BA was synthesized (Table 1, entry 21). First, PIBA block was prepared (Table 1, entry 1) using normal ATRP and then used as a macroinitiator. Extension with *n*BA was efficient. Fig. 2 presents the SEC chromatograms recorded after each step. The reactions were well controlled, as evidenced by the GPC traces being monomodal, and final block copolymer was formed with a low polydispersity (PDI = 1.12), although small tailing was observed.

3.1.2. Synthesis of gradient copolymer

The third class of copolymer was a gradient copolymer P(IBA-*grad*-*n*BA). Gradient copolymers form a completely new class of polymers with well-defined structure and composition. They exhibit a gradual change of composition from predominantly one comonomer to the other, as a function of copolymer chain length. In general, two methods can be applied in the synthesis of gradient copolymers using ATRP system [29]. The first one is the use of *batch copolymerization*, in which a spontaneous gradient in instantaneous composition is formed, based on differences in the reactivity ratios of the comonomers in the monomer feed [34–37]. The second is the use of *semi-batch copolymerization* to form controlled gradients in instantaneous composition (forced gradient method). In this method, the formation of gradient is influenced by continuous change in monomer feed caused by addition of the monomer [38–42]. Since reactivity ratios of *n*BA and IBA are similar, a semi-batch copolymerization method was used in order to obtain gradient structure.

A continuous gradient was targeted (100% *n*BA on one side of the polymer chain to 90% IBA on the other) for P(IBA-*grad*-*n*BA) copolymer. Under this condition, the rate at which the second monomer (IBA) was added had to be synchronized with the polymerization rate of the first one (*n*BA). Thus, after performing the test homopolymerization of *n*BA, the following approach was chosen to synthesize P(IBA-*grad*-*n*BA). A primary polymerization of *n*BA was performed under ATRP conditions (*n*BA/EtBrIB/CuBr/$CuBr_2$/PMDETA = 307/1/2/0.1/2.1; in anisole 0.25 vol. equivalent vs. *n*BA; $T = 50$ °C). Through constant addition (0.86 ml/h) of IBA (secondary mixture: IBA/CuBr/$CuBr_2$/PMDETA = 192/2/0.1/2.1 in DPE 0.25 vol. equivalent vs. IBA) to the primary mixture, the feed ratio was continuously shifted from 100% *n*BA in the beginning to 82% IBA at the end of polymerization. In comparison to homopolymerization of *n*BA, one half of *n*BA was substituted by IBA. Two different solvents were used (anisole and DPE) to follow conversions of both monomers by GC. To avoid a significant decrease in the polymerization rate, catalyst was added along with second comonomer (secondary mixture).

Fig. 3 shows the change of concentration of both monomers during gradient copolymerization. Kinetic data were obtained by measuring monomers conversion by GC relative to internal standards (anisole, DPE). In the early stage of polymerization, fast consumption of *n*BA was observed. This is the result of the high concentration of initiator and low concentration of

Table 1
Properties of various acrylate (co)polymers prepared by ATRP[a]

Entry	Sample name	Type of copolymer	M1 (DP = X)	M2 (DP = Y)	M1 wt% (GC)	T_g predicted[b]	M1 wt% (NMR)	GPC results		$M_{n,\ theor}$[c]
								PDI	M_n	
1	WJ-02-09	Homopolymer	IBA (DP = 290)	–	100	94.0	–	1.06	28 500	35 400
2	WJ-02-11	Homopolymer	*t*BA (DP = 470)	–	100	43.0	–	1.07	48 900	43 800
3	WJ 135	Homopolymer	MA (DP = 630)	–	100	10.0	–	1.16	42 200	40 000
4	WJ-02-07	Homopolymer	EA (DP = 900)	–	100	−24.0	–	1.06	96 900	70 200
5	WJ-02-29	Homopolymer	*n*PA (DP = 700)	–	100	−40.0		1.06	86 000	58 800
6	WJ-02-10	Homopolymer	*n*BA (DP = 460)	–	100	−54.0	–	1.07	47 900	40 800
7	WJ-02-13	Statistical	IBA (DP = 240)	*n*BA (DP = 100)	80	46.5	79	1.06	34 000	48 000
8	WJ-02-19	Statistical	IBA (DP = 480)	*n*BA (DP = 200)	80	46.5	78	1.08	63 700	66 000
9	WJ-02-14	Statistical	IBA (DP = 150)	*n*BA (DP = 245)	50	7.0	53	1.05	43 500	51 600
10	WJ-02-20	Statistical	IBA (DP = 300)	*n*BA (DP = 490)	50	7.0	54	1.06	69 000	67 000
11	WJ-02-35	Statistical	IBA (DP = 41)	*n*BA (DP = 90)	43	−10.6	41	1.08	26 300	18 400
12	WJ-02-36	Statistical	IBA (DP = 82)	*n*BA (DP = 180)	43	−10.6	39	1.07	39 700	31 600
13	WJ-02-28	Statistical	IBA (DP = 165)	*n*BA (DP = 360)	43	−10.6	44	1.07	53 000	48 800
14	WJ-02-24	Statistical	IBA (DP = 245)	*n*BA (DP = 540)	43	−10.6	42	1.10	100 500	92 400
15	WJ-02-16	Statistical	IBA (DP = 110)	*n*BA (DP = 315)	35	−20.4	38	1.06	44 300	45 000
16	WJ-02-22	Statistical	IBA (DP = 220)	*n*BA (DP = 630)	35	−20.4	33	1.12	107 500	92 400
17	WJ-02-15	Statistical	IBA (DP = 60)	*n*BA (DP = 390)	20	−32.7	19	1.05	44 700	44 400
18	WJ-02-21	Statistical	IBA (DP = 120)	*n*BA (DP = 780)	20	−32.7	22	1.07	81 900	76 800
19	WJ-02-17	Statistical	IBA (DP = 30)	*n*BA (DP = 440)	10	−41.9	13	1.06	55 600	45 000
20	WJ-02-23	Statistical	IBA (DP = 60)	*n*BA (DP = 880)	10	−41.9	16	1.13	94 000	76 900
21	WJ-02-30	Block	WJ-02-09	*n*BA (DP = 470)	50	94, −54	54	1.12	54 600	46 300
22	WJ-02-45	Gradient	IBA (DP = 192)	*n*BA (DP = 307)	47	–	47	1.13	74 800	62 300

[a] Typical ATRP conditions: M1/M2/EtBrIB/CuBr/PMDETA = X/Y/1/2/2; in acetone/anisole (0.25/0.05 vol. equivalent vs. M1), $T = 50$ °C.
[b] Predicted using Fox equation.
[c] $M_{n,\ theor} = ([M]_0/[In]_0) \times$ conversion $\times M_{monomer}$; DP = degree of polymerization.

competing IBA. During the reaction, polymerization of *n*BA slows down due to dilution with IBA. The polymerization rate of IBA increases due to the higher molar ratio in the feed. After finishing the addition of IBA (5.4 h), 87% of *n*BA was polymerized and 62% of IBA was consumed. The polymerization was continued for 1 h after the addition of second comonomer was completed. The polymerization still proceeded after the monomer addition was stopped and resulted

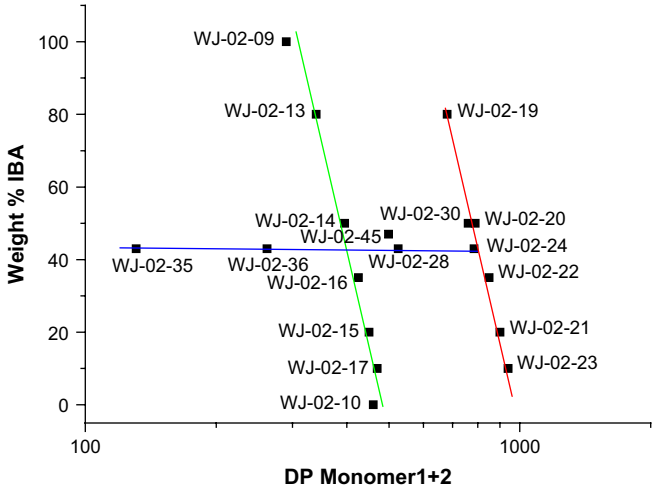

Scheme 2. Schematic representation of prepared copolymer samples of P(IBA-*co*-*n*BA) with different molecular weights and compositions (Table 1 presents detailed characterization of all copolymers). (For interpretation of the references to color in this scheme legend, the reader is referred to the web version of this article.)

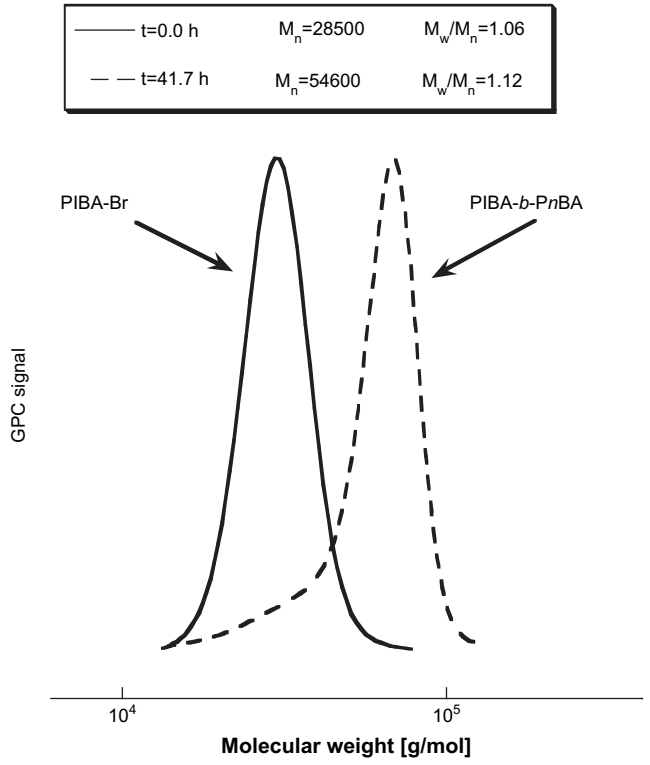

Fig. 2. GPC traces after each step of synthesis of block copolymers PIBA-*b*-P*n*BA. Experimental conditions for polymerization of IBA: IBA/EtBrIB/CuBr/PMDETA = 290/1/1/1 in acetone/anisole (0.25/0.05 vol. equivalent vs. M1), $T = 50$ °C. Experimental conditions for polymerization of *n*BA: *n*BA/PIBA/CuBr/PMDETA = 470/1/2/2 in acetone/anisole (1.0/0.1 vol. equivalent vs. M1), $T = 50$ °C.

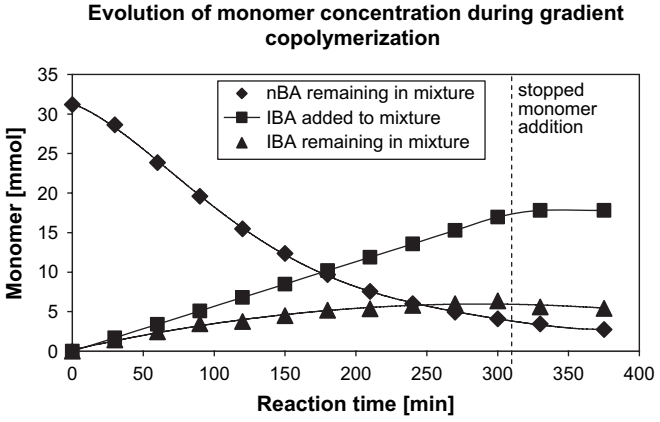

Fig. 3. Evolution of monomer concentration during gradient copolymerization of IBA and *n*BA.

in a short statistical copolymer block at the end of the gradient copolymer.

GPC traces of samples taken every hour are shown in Fig. 4a. The curves shift smoothly to higher molecular weights. Final polydispersity was low (<1.2) and decreased during the polymerization, indicating that polymerization was well controlled. In Fig. 4b the theoretical molecular weights (calculated from conversion data obtained from GC measurements) are compared to the experimental values determined by GPC. With the reaction time difference between $M_{n,\,GPC}$ and $M_{n,\,theor}$ is increasing. This is probably due to different hydrodynamic volumes of gradient copolymer and PMMA standards. This difference increases with the amount of IBA incorporated into the copolymer.

Fig. 5 shows instantaneous composition of P(IBA-*grad*-*n*BA). The average, instantaneous composition in each segment decreases continuously from 100% *n*BA in the beginning of the average polymer chain to 22% at the end. These data confirm the gradient structure of final copolymer. The overall composition was *n*BA/IBA = 69/31 (mol%).

3.2. Thermomechanical properties and morphology

3.2.1. Statistical P(IBA-co-nBA) copolymers

When comparing the thermomechanical properties of acrylate homopolymers and P(IBA-*co*-*n*BA) copolymers, the first important question is whether the copolymer system is isotropic in the bulk state or rather exhibits a micro-phase separation. To answer this question the DSC thermographs for all samples described in Table 1 were measured. Some typical results obtained from statistical copolymers with different compositions (the green line) together with the respective curves for PIBA and P*n*BA homopolymers are shown in Fig. 6. Clearly, all the copolymers are completely amorphous and exhibit only a single glass transition at a temperature increasing with the increase of the IBA content. This indicates that there is no micro-phase separation in the statistical P(IBA-*co*-*n*BA) copolymers, a finding further confirmed by DMA and SAXS experiments, which will be discussed below.

The T_g's of all statistical copolymers (from the green and red lines in Scheme 2) are plotted vs. their IBA content in Fig. 7. The T_g varies continuously with composition in both low and high molecular weight samples. To describe such type of composition dependence of the T_g of copolymers or miscible polymer blends, the so-called Fox equation was used [43]:

$$\frac{1}{T_g} = \frac{w_1}{T_{g1}} + \frac{w_2}{T_{g2}}$$

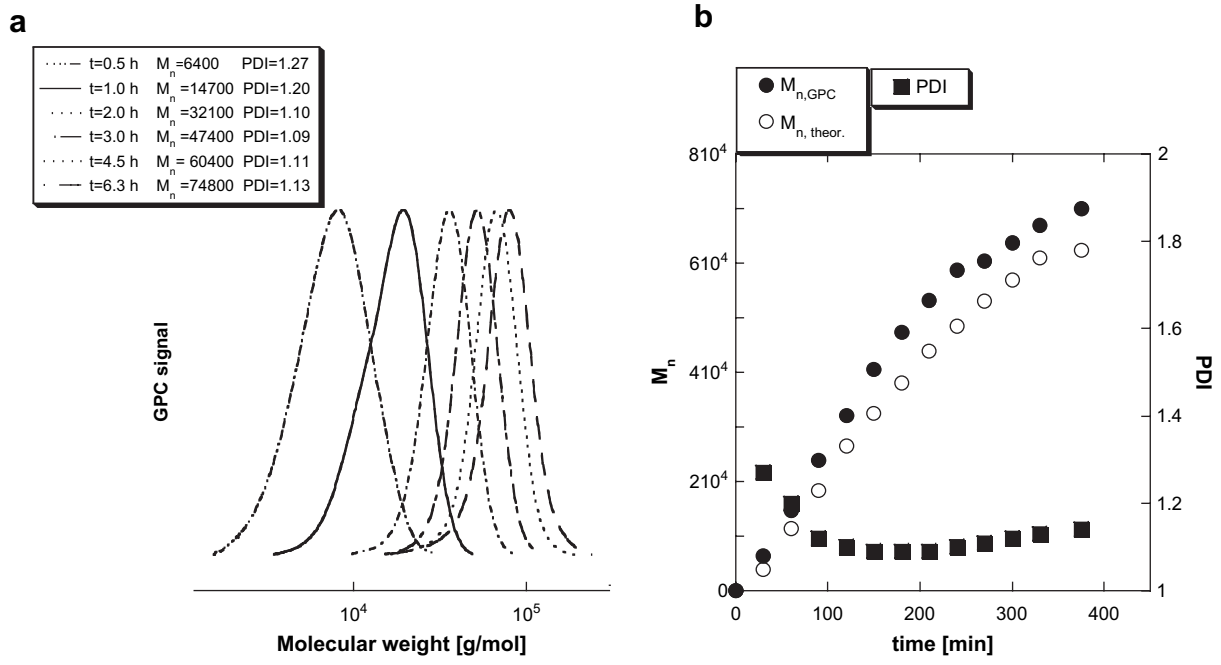

Fig. 4. (a) Evolution of M_n GPC traces and (b) molecular weights and polydispersities as a function of conversion during gradient copolymerization of IBA and *n*BA (conditions for the reaction, see Section 2).

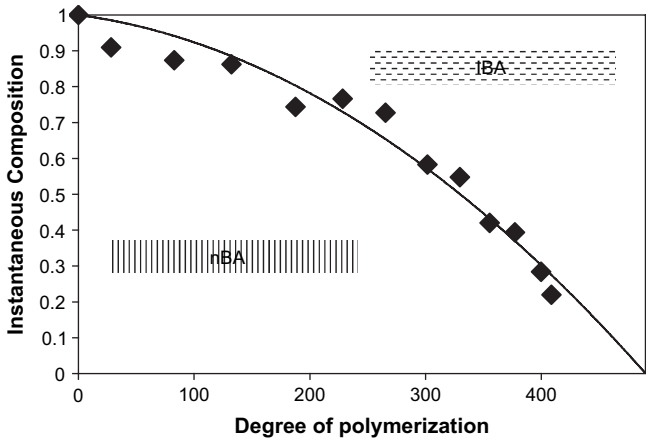

Fig. 5. Instantaneous composition of gradient copolymer P(IBA-*grad*-*n*BA).

where T_g is the glass transition temperature of the copolymer, T_{g1} and T_{g2} are the glass transition temperatures of the two homopolymers, and w_1 and w_2 are the weight fractions of the two repeat units in the copolymer. As can be seen in Fig. 7, the experimentally measured T_g values closely follow the predictions of the Fox equation, which is represented by the line linking the two homopolymers' T_gs.

Dynamic mechanical analysis (DMA) was used to study the influence of the composition on the dynamics of the P(IBA-*co*-*n*BA) copolymers. In Fig. 8 the frequency dependence of the real (G') and imaginary (G'') parts of the shear modulus (master curves) are presented for a series of statistical copolymers with similar (low) degree of polymerization and an increasing amount of the IBA content (the green line in Scheme 2). It is important to emphasize that all statistical copolymers studied here, allowed for a construction of a smooth master curves and the shift factors conform to the WLF equation. This confirms

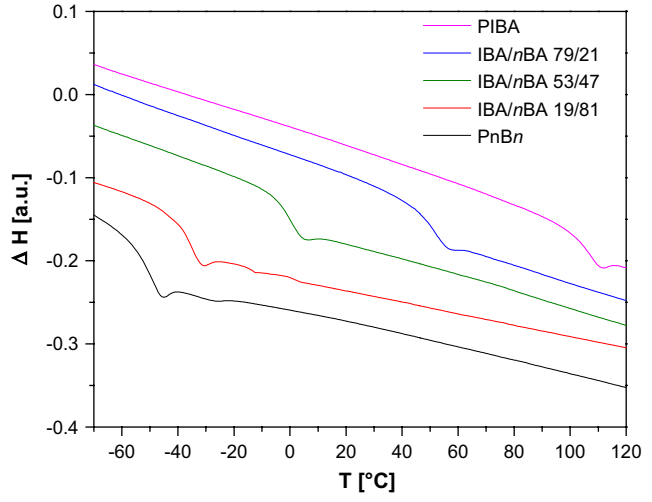

Fig. 6. DSC thermograms of statistical P(IBA-*co*-*n*BA) copolymers with different monomer compositions: IBA(19%)–*n*BA(81%) copolymer (red, WJ-02-15), IBA(53%)–*n*BA(47%) copolymer (green, WJ-02-14), IBA(79%)–*n*BA(21%) copolymer (blue, WJ-02-13) of IBA and *n*BA. The thermographs of the respective homopolymers are also shown for comparison (black for *n*BA and pink for IBA, respectively). (For interpretation of the references to color in this figure legend, the reader is referred to the web version of this article.)

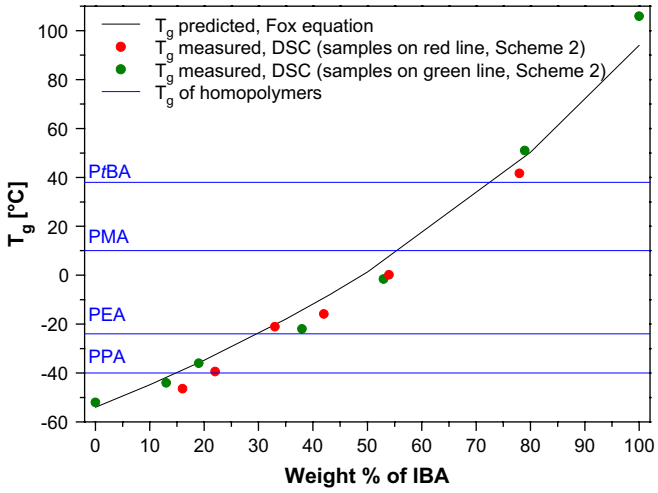

Fig. 7. Tuning T_g in statistical copolymers of P(IBA-*co*-*n*BA) with different IBA/*n*BA ratios and two different degrees of polymerization (Scheme 2, copolymers on green and red line).

that the statistical P(IBA-*co*-*n*BA) copolymers obey the principle of time–temperature superposition, i.e., they can be considered as thermorheologically simple. This subject can be addressed more quantitatively by analyzing the temperature dependence of the minimum of tan(δ), as recently shown for a series of cycloolefin copolymers with different norbornene content [44]. Such analyses, however, are beyond the scope of this paper.

Let us first consider the pure P*n*BA. As can be seen in Fig. 8, the relaxation spectrum of this homopolymer shows two distinct characteristic regions. The one at high frequencies is related to segmental (local) motions of the polymer chains and the lower frequency, or terminal one, is related to relaxation of entangled chains. These two parts of the spectra are characterized with their respective relaxation times, τ_s and τ_c [45]. These relaxation times determine the time range within which the characteristic rubbery plateau is observed

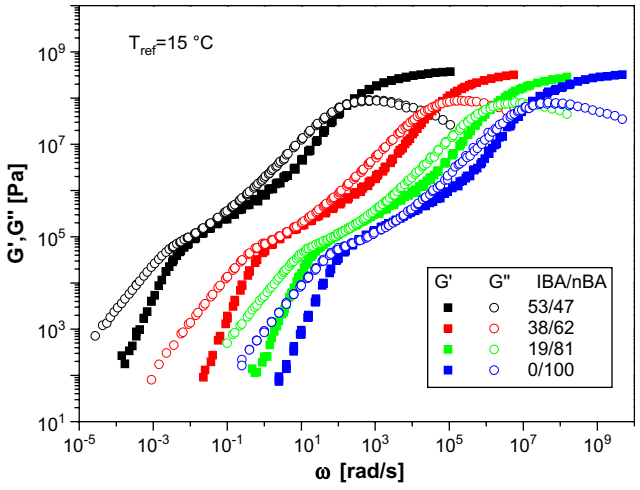

Fig. 8. Typical examples of G' and G'' dependencies (master curves) on frequency for a linear P*n*BA homopolymer and statistical P(IBA-*co*-*n*BA) copolymers with similar degrees of polymerization and different IBA/*n*BA ratios (Scheme 2, the green line).

for linear polymers. For most of the linear flexible polymers, as well as for P*n*BA, the plateau height is between 10^5 and 10^6 Pa. Outside the rubbery plateau range the linear polymer melts become glassy at high frequencies and flow within longer time periods, i.e., at low frequencies.

As can be seen from Fig. 8, the increased amount of IBA in the copolymer composition leads to a systematic shift of the master curves to lower frequencies. This effect is related to the strong increase of the glass transition temperatures of the respective copolymers. However, the shape of the master curves does not change significantly and there is no evidence of any new relaxation processes in the copolymers as compared to a P*n*BA homopolymer. This is an additional indication that the statistical P(IBA-*co*-*n*BA) copolymers do not exhibit a phase separation. In order to better understand the influence of the composition on the dynamics of the statistical copolymers, we have determined the characteristic times t_c related to the terminal relaxation process by the crossing points of the G' and G'' curves observed at the transition to the flow range at low frequency. Results are shown in Fig. 9a as a function of the IBA content for the copolymers from the green and the red line in Scheme 2. As in earlier study [46] the terminal relaxation times are normalized to the relaxation times of the segmental motion, which makes the results nearly independent of the reference temperature and free of effects related to the chain length dependence of the segmental motion, usually observed for short chains.

As can be seen in Fig. 9a, the terminal relaxation times of the copolymers depend weakly on the IBA content and much stronger on the degree of polymerization. Furthermore even this weak dependence is most likely related to the slight decrease of the copolymers molecular weight with the decrease of IBA content (see Table 1). This is further illustrated in Fig. 9b where the same data are plotted versus the molecular weight of the copolymers. For comparison, the data for statistical copolymers with similar composition but different degree of polymerization (the blue line on Scheme 2) are also shown. All statistical copolymers show similar molecular weight dependence of the terminal relaxation times independent of their composition. The slope of this dependence is approximately 4, a value slightly higher than that typically found for homopolymer melts in the entangled regime, i.e., ~3.4.

3.3. Comparison of the statistical P(IBA-co-nBA) copolymers with acrylate homopolymers

As shown in a previous section, the glass transition of the statistical P(IBA-*co*-*n*BA) copolymers can be tuned to any value between the T_g's of the two homopolymers (i.e., between −54 and 94 °C) by proper choice of the comonomer ratio. It is possible therefore, to synthesize copolymers with glass transition temperatures matching the T_g of other acrylate homopolymers. This is illustrated in Fig. 7, where the glass transition temperatures of the PPA, PEA, PMA and P*t*BA are shown as horizontal lines. It is interesting to verify if the statistical P(IBA-*co*-*n*BA) copolymers can mimic not only the T_g's of the acrylate homopolymers, but also their mechanical properties. In order to do this, we plotted in Fig. 10a the DMA master curves measured for PPA homopolymer and IBA(16%)−*n*BA(84%) copolymer with similar molecular weight. The two master curves overlap very well both in the high frequency region (due to the similar T_gs) and in the low frequency region (due to the similar M_n). Nevertheless, a closer look at Fig. 10a reveals also some differences.

Most importantly, in the characteristic rubbery plateau region the storage modulus (G') of the P(IBA-*co*-*n*BA) copolymer is significantly lower than the corresponding value for the PPA homopolymer. This effect is even more evident in Fig. 10b, which compares the master curve of statistical copolymer with IBA(33%)/*n*BA(67%) with that of the PEA homopolymer of similar molecular weight. Again, the overlap of the two spectra is remarkably good at high and low frequencies, but the significant difference in the storage modulus is observed in the plateau region. This means that while mimicking perfectly the glass transition temperatures of the PEA and PPA, the P(IBA-*co*-*n*BA) copolymers are significantly softer than their homopolymer counterparts. It is interesting to verify if similar observations can be made also when comparing the copolymers with higher IBA content, i.e., higher glass transition temperature with the PMA and P*t*BA homopolymers. Unfortunately, as can be seen from Fig. 7, none of the synthesized copolymers had the appropriate composition in order to match the T_g of the PMA. Nevertheless, the IBA(78%)−*n*BA(22%) copolymer (WJ-02-19) has a glass transition temperature very similar to that of the P*t*BA. The DMA master curves of

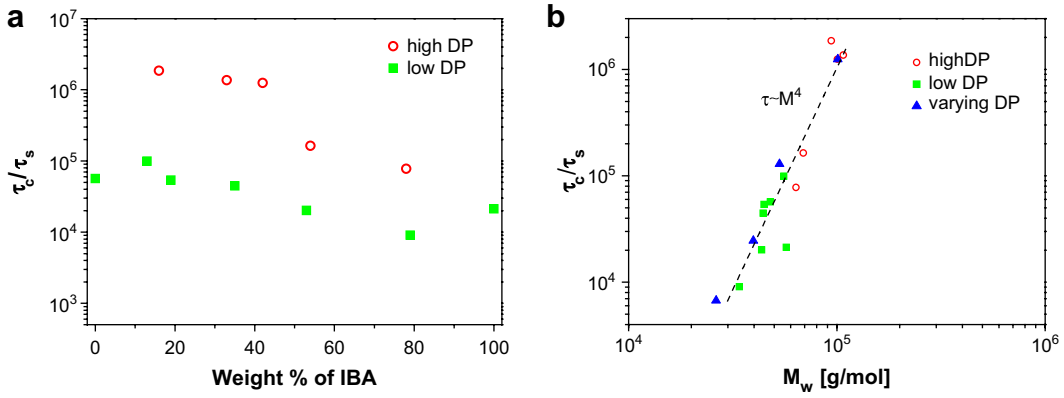

Fig. 9. Effect of the composition (a) and the molecular weight (b) of statistical copolymers P(IBA-*co*-*n*BA) on the chain relaxation times.

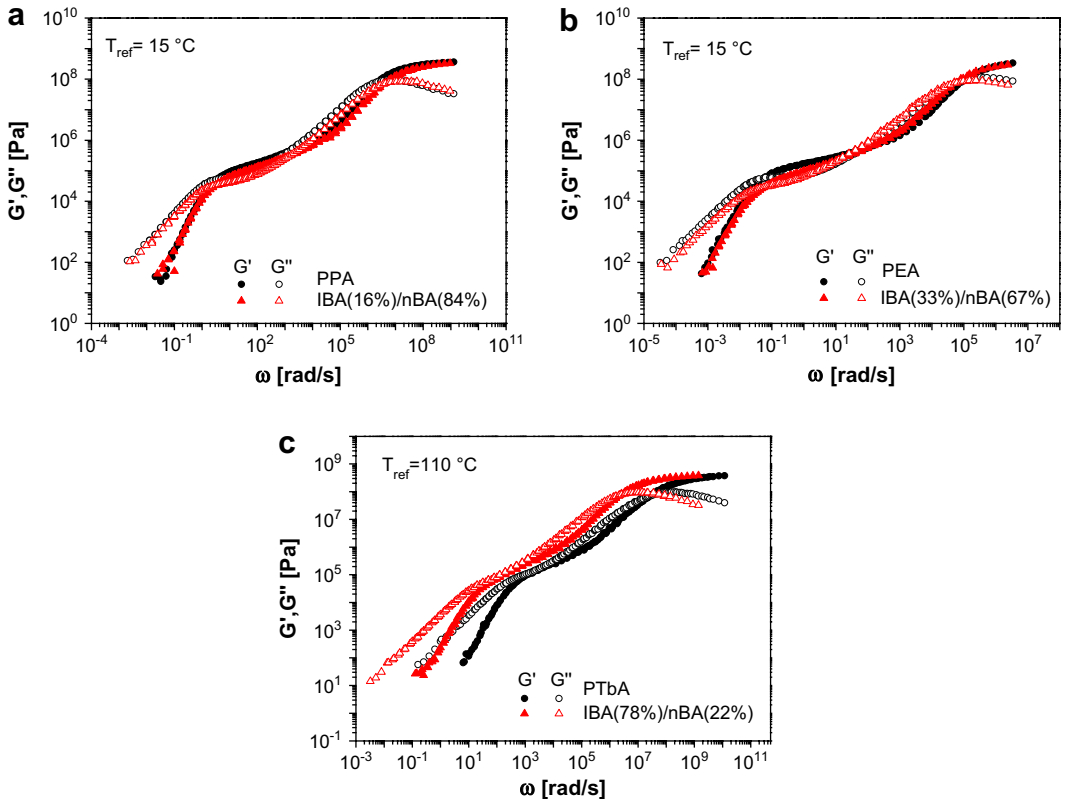

Fig. 10. Comparison of the shear moduli spectra of (a) PPA ($T_g = -40$ °C, $M_n = 86\,000$ g/mol; WJ-02-29) and IBA(16%)–*n*BA(84%) copolymer ($T_g = -39$ °C, $M_n = 94\,000$ g/mol; WJ-02-23); (b) PEA ($T_g = -24$ °C, $M_n = 96\,900$ g/mol; WJ-02-07) and IBA(33%)–*n*BA(67%) copolymer ($T_g = -20$ °C, $M_n = 107\,500$ g/mol; WJ-02-22); (c) P*t*BA ($T_g = 37$ °C, $M_n = 48\,900$ g/mol; WJ-02-11) and IBA(78%)–*n*BA(22%) copolymer ($T_g = 42$ °C, $M_n = 63\,700$ g/mol; WJ-02-19).

these two materials are shown in Fig. 10c. The spectra are very similar although slightly shifted due to the small difference in the glass transition temperatures. More importantly, the copolymer is again softer than the homopolymer, i.e., has a lower G' value in the rubbery plateau region. The data for the G' in this region for all materials presented in Fig. 10 are summarized in Table 2. For comparison the values for *n*BA and IBA homopolymers are also shown. As can be seen from the table in all cases, the P(IBA-*co*-*n*BA) copolymers are significantly softer than the respective homopolymers having same glass transition temperatures. The lower plateau modulus of the copolymers indicates that they should have higher entanglement M_w. The effect is most likely related to the rather big and rigid side group of IBA, which prevents the copolymer chains from a denser packing and therefore results in a less dense and softer IBA containing copolymers. This conclusion is further confirmed by the very low plateau modulus of the IBA homopolymer itself.

Table 2
Glass transition temperature and rubbery plateau storage modulus for the polymers shown in Fig. 10

Polymer	Sample name	T_g (°C)	Plateau G' (kPa)
PPA	WJ-02-29	−40	140
IBA(16%)–*n*BA(84%)	WJ-02-23	−39	95
PEA	WJ-02-07	−24	170
IBA(33%)–*n*BA(67%)	WJ-02-22	−20	70
P*t*BA	WJ-02-11	37	135
IBA(78%)–*n*BA(22%)	WJ-02-19	42	85
*n*BA	WJ-02-10	−54	130
IBA	WJ-02-09	105	80

3.4. Gradient P(IBA-grad-nBA) and block PIBA-b-PnBA copolymers

As discussed above, the statistical P(IBA-*co*-*n*BA) copolymers exhibit "homopolymer type" thermomechanical properties, with no evidence for a two phase behavior. However, the situation is remarkably different in the case of gradient and especially block copolymers. In order to illustrate this, Fig. 11a compares the DSC thermographs of a statistical copolymer and a gradient copolymer, with similar IBA/*n*BA composition and comparable molecular weight. As expected, the statistical copolymer shows a clear glass transition at a temperature between the T_g's of the two homopolymers in agreement with the Fox equation. The gradient copolymer, however, reveals a broad glass transition region with no obvious glass transition temperature [28–30]. Such behavior is probably caused by the broad distribution of IBA and *n*BA segments with different lengths along the gradient copolymer chains.

Similar conclusions may be derived from the results of the DMA measurements illustrated in Fig. 11b. The master curve for the statistical copolymer shows the two distinct characteristic relaxation regions, as expected. The master curve for the gradient copolymer, however, shows very broad distribution of

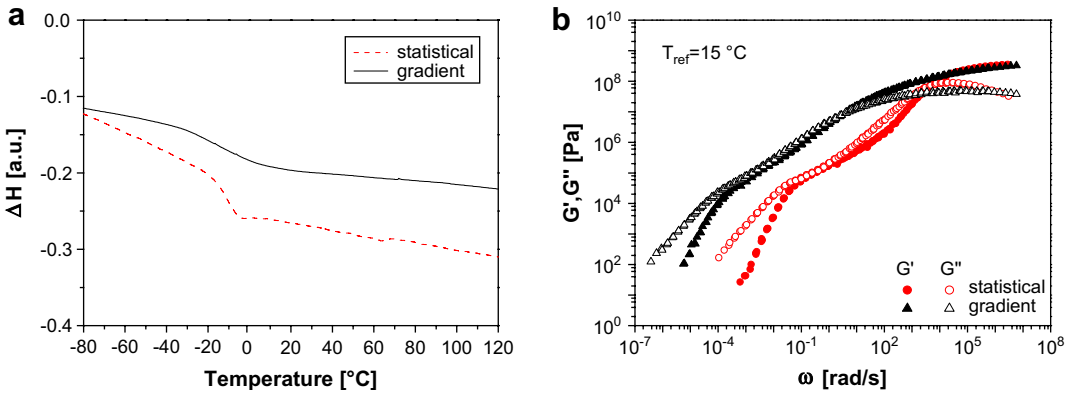

Fig. 11. Comparisons between gradient IBA(47%)–*n*BA(53%) copolymer (broad T_g, $M_n = 74\,800$ g/mol; WJ-02-45) and statistical IBA(44%)–*n*BA(56%) copolymer ($T_g = -10.6$ °C, $M_n = 53\,000$ g/mol; WJ-02-28).

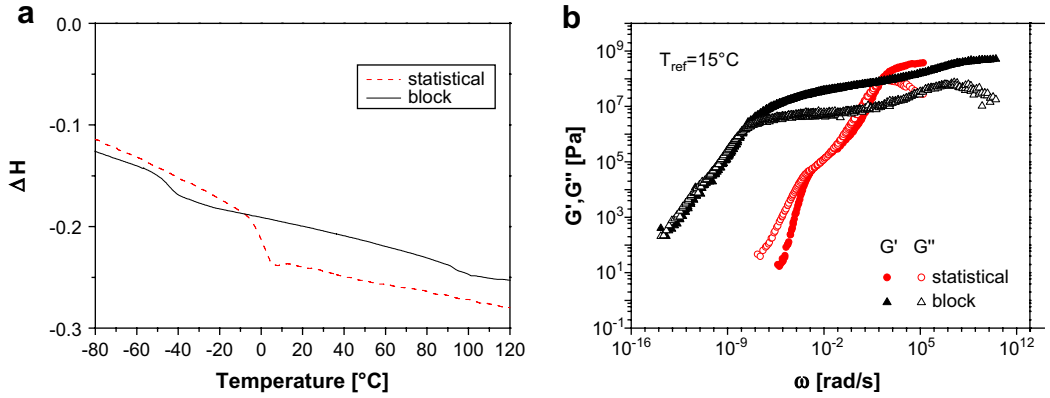

Fig. 12. Comparisons of block IBA(54%)–*n*BA(46%) copolymer ($T_g = -54$ °C, 94 °C, $M_n = 54\,600$ g/mol; WJ-02-230) and statistical IBA(54%)–*n*BA(46%) copolymer ($T_g = 7$ °C, $M_n = 69\,000$ g/mol; WJ-02-20).

relaxation processes, particularly in the segmental relaxation region. It was previously reported that this broadening could be related to compositions' fluctuations in the studied copolymers [47,48]. A recent study of a similar system has shown that using experimental techniques such as photon correlation spectroscopy and dielectric spectroscopy the relaxation dynamic can be addressed in greater details [49].

In Fig. 12a, the DSC thermographs of statistical and block copolymers with similar molecular weight and similar IBA/*n*BA composition are compared. While, the statistical copolymer has a single glass transition, the block copolymer shows two glass transition temperatures corresponding to the T_g's of each component indicating a micro-phase separation in the sample. In Fig. 12b the frequency dependence of G' and G'' of the same copolymers are compared. It is important to emphasize that in the case of the block copolymer, merely an attempt for constructing a master curve is shown, as the temperature dependence of the shift factors does not conform to the WLF equation. Nevertheless such an approach was shown to reveal important information for the morphology and order–disorder transitions in a number of block copolymer systems [50–52]. In our case, the block copolymer "master curve" provides additional evidences for the micro-phase separation in this sample. First of all the glass transitions of the two blocks are clearly distinguishable at low and high frequencies, respectively. Furthermore the behavior of the "master curve" in the very low frequency region, namely $G'(\omega)$ overlapping with $G''(\omega)$ and having a slope of ~ 0.5 may indicate the formation of a lamella structure as theoretically predicted [53].

In order to verify these findings, SAXS experiments were performed on the same pair of block and statistical copolymers. As expected the statistical copolymer has revealed a smooth scattered intensity distribution without any peaks. The block copolymer, however, showed a week maxima, which may result from distance correlations between P*n*BA and PIBA domains. There are no other peaks in the spectra probably as result of the small contrast in the electronic densities of the two blocks. For this reason it is not possible to make any conclusions concerning type of order or to identify any specific morphological forms. From the position of the maxima, however, a structural periodicity of ≈ 20 nm can be assigned to the block copolymer sample.

4. Conclusions

In summary, block, statistical and gradient copolymers built with IBA and *n*BA units were successfully synthesized using the ATRP process. All polymers were prepared with controlled molecular weight and narrow molecular weight distribution.

Statistical copolymers were synthesized with various IBA/*n*BA compositions and molecular weights. Their thermomechanical properties were investigated and compared to block, gradient copolymers and to P*n*PA, PEA, PMA and P*t*BA homopolymers. By the proper choice of the IBA/*n*BA monomer ratio, it was possible to tune the glass transition temperature of the statistical P(IBA-*co*-*n*BA) copolymers. Measured T_gs fitted well with the Fox equation prediction. Thus, it was possible to generate materials based on IBA/*n*BA copolymers that can mimic thermal properties of homopolymers such as PMA, PEA, P*n*PA or P*t*BA. However, the mechanical properties of the statistical copolymers differed significantly from their homopolymer equivalents. DMA analysis revealed that the P(IBA-*co*-*n*BA) copolymers were softer than the respective homopolymers having same glass transition temperatures.

While statistical copolymers showed a single glass transition (T_g between −50 and 90 °C depending on composition), block copolymers showed two T_gs and DSC thermograms for the gradient copolymer indicated a single, but very broad, glass transition. The mechanical properties of block and gradient copolymers were very different from that of the statistical copolymers with the same composition. Thus, the different arrangements of IBA and *n*BA units along a polymer chain affected significantly thermal and mechanical properties of the final copolymers.

When searching for new materials, the investigation on systems built with two or more components is in demand, especially for structure–property correlation. Presented results showed that only by changing arrangement of two different monomer units, one can obtain materials with significantly different properties. Two component systems can be used to mimic, in this case, thermal properties of one-component materials but at the same time may have significantly different mechanical properties. In a similar way, one can copolymerize other monomers and affect not only physical properties of final polymer materials but also their degradation rates and toxicity, both of which might be important, for example, in biomedical applications.

Acknowledgment

The authors thank the National Science Foundation (DMR-05-49353) and the members of the CRP Consortium at Carnegie Mellon University for their financial support.

References

[1] Matyjaszewski K, Gnanou Y, Leibler L. Macromolecular engineering. Precise synthesis, materials properties, applications. Weinheim: Wiley-VCH; 2007.
[2] Leibler L. Prog Polym Sci 2005;30(8–9):898–914.
[3] Choi HS, Yui N. Prog Polym Sci 2006;31(2):121–44.
[4] Frechet JMJ. Prog Polym Sci 2005;30(8–9):844–57.
[5] Higgins JS, Tambasco M, Lipson JEG. Prog Polym Sci 2005;30(8–9):832–43.
[6] Khandare J, Minko T. Prog Polym Sci 2006;31(4):359–97.
[7] Macosko CW, Jeon HK, Hoye TR. Prog Polym Sci 2005;30(8–9):939–47.
[8] Meijer HEH, Govaert LE. Prog Polym Sci 2005;30(8–9):915–38.
[9] Sukhorukov G, Fery A, Moehwald H. Prog Polym Sci 2005;30(8–9):885–97.
[10] Various controlled/living polymerizations and their application to the synthesis of block copolymers are covered in the following review articles:
(a) Matyjaszewski K, Müller AHE. Prog Polym Sci 2006;31:1039–40;
(b) Smid J, Van Beylen M, Hogen-Esch TE. Prog Polym Sci 2006;31:1041–67;
(c) Hadjichristidis N, Iatrou H, Pitsikalis M, Mays J. Prog Polym Sci 2006;31:1068–132;
(d) Yagci Y, Tasdelen MA. Prog Polym Sci 2006;31:1133–70;
(e) Bielawski CW, Grubbs RH. Prog Polym Sci 2007;32:1–29;
(f) Domski GJ, Rose JM, Coates GW, Bolig AD, Brookhart M. Prog Polym Sci 2007;32:30–92;
(g) Braunecker WA, Matyjaszewski K. Prog Polym Sci 2007;32:93–146;
(h) Yokozawa T, Yokoyama A. Prog Polym Sci 2007;32:147–72;
(i) Baskaran D, Mueller AHE. Prog Polym Sci 2007;32:173–219;
(j) Goethals EJ, Du Prez F. Prog Polym Sci 2007;32:220–46;
(k) Penczek S, Cypryk M, Duda A, Kubisa P, Slomkowski S. Prog Polym Sci 2007;32:247–82.
[11] Matyjaszewski K, Spanswick J. Mater Today 2005;8(3):26–33.
[12] Matyjaszewski K, Davis TP. Handbook of radical polymerization. Hoboken: Wiley Interscience; 2002.
[13] Matyjaszewski K, Xia J. Chem Rev 2001;101(9):2921–90.
[14] Kamigaito M, Ando T, Sawamoto M. Chem Rev 2001;101(12):3689–745.
[15] Tsarevsky NV, Matyjaszewski K. Chem Rev 2007;107(6):2270–99.
[16] Georges MK, Veregin RPN, Kazmaier PM, Hamer GK. Macromolecules 1993;26(11):2987–8.
[17] Hawker CJ, Bosman AW, Harth E. Chem Rev 2001;101(12):3661–88.
[18] Chiefari J, Chong YK, Ercole F, Krstina J, Jeffery J, Le TPT, et al. Macromolecules 1998;31(16):5559–62.
[19] Qiu J, Charleux B, Matyjaszewski K. Prog Polym Sci 2001;26(10):2083–134.
[20] Coessens V, Pyun J, Miller PJ, Gaynor SG, Matyjaszewski K. Macromol Rapid Commun 2000;21(2):103–9.
[21] Patten TE, Matyjaszewski K. Adv Mater (Weinheim, Ger.) 1998;10(12):901–15.
[22] Wang J-S, Matyjaszewski K. J Am Chem Soc 1995;117(20):5614–5.
[23] Matyjaszewski K. J Macromol Sci Pure Appl Chem 1997;A34(10):1785–801.
[24] Matyjaszewski K. Macromolecules 1998;31(15):4710–7.
[25] Davis KA, Matyjaszewski K. Statistical, gradient, block and graft copolymers by controlled/living radical polymerizations. Adv Polym Sci 2002;159:2–166.
[26] Ziegler MJ, Matyjaszewski K. Macromolecules 2001;34(3):415–24.
[27] Arehart SV, Matyjaszewski K. Macromolecules 1999;32(7):2221–31.
[28] Matyjaszewski K, Shipp DA, McMurtry GP, Gaynor SG, Pakula T. J Polym Sci Part A Polym Chem 2000;38(11):2023–31.
[29] Matyjaszewski K, Ziegler MJ, Arehart SV, Greszta D, Pakula T. J Phys Org Chem 2000;13(12):775–86.
[30] Kim J, Mok MM, Sandoval RW, Woo DJ, Torkelson JM. Macromolecules 2006;39(18):6152–60.
[31] Gray MK, Zhou H, Nguyen ST, Torkelson JM. Macromolecules 2004;37(15):5586–95.
[32] Brandrup J, Immergut EH, Grulke EA. Polymer handbook. 4th ed. New York: Wiley-Interscience; 1999.
[33] Xia J, Matyjaszewski K. Macromolecules 1997;30(25):7697–700.
[34] Min K, Li M, Matyjaszewski K. J Polym Sci Part A Polym Chem 2005;43(16):3616–22.
[35] Qin S, Saget J, Pyun J, Jia S, Kowalewski T, Matyjaszewski K. Macromolecules 2003;36(24):8969–77.
[36] Lee H-I, Matyjaszewski K, Yu S, Sheiko SS. Macromolecules 2005;38(20):8264–71.
[37] Lee SB, Russell AJ, Matyjaszewski K. Biomacromolecules 2003;4(5):1386–93.

[38] Min K, Oh JK, Matyjaszewski K. J Polym Sci Part A Polym Chem 2007;45(8):1413–23.
[39] Boerner HG, Duran D, Matyjaszewski K, da Silva M, Sheiko SS. Macromolecules 2002;35(9):3387–94.
[40] Sun X, Luo Y, Wang R, Li B-G, Liu B, Zhu S. Macromolecules 2007;40(4):849–59.
[41] Wang R, Luo Y, Li B-G, Zhu S. AIChE J 2007;53(1):174–86.
[42] Wang R, Luo Y, Li B, Sun X, Zhu S. Macromol Theory Simul 2006; 15(4):356–68.
[43] Fox TG. Bull Am Phys Soc 1956;1:123.
[44] Blochowiak M, Pakula T, Butt HJ, Bruch M, Floudas G. J Chem Phys 2006;124(13):134903/1–134903/8.
[45] Pakula T, Geyder S, Edling T, Boese D. Rheol Acta 1996;35(6): 631–44.
[46] Zhang Y, Chung IS, Huang J, Matyjaszewski K, Pakula T. Macromol Chem Phys 2005;206(1):33–42.
[47] Karatasos K, Anastasiadis SH, Floudas G, Fytas G, Pispas S, Hadjichristidis N, et al. Macromolecules 1996;29(4):1326–36.
[48] Kumar SK, Colby RH, Anastasiadis SH, Fytas G. J Chem Phys 1996; 105(9):3777–88.
[49] Alvarez F, Colmenero J, Wang CH, Xia JL, Fytas G. Macromolecules 1995;28(19):6488–93.
[50] Floudas G, Ulrich R, Wiesner U. J Chem Phys 1999;110(1):652–63.
[51] Floudas G, Pispas S, Hadjichristidis N, Pakula T, Erukhimovich I. Macromolecules 1996;29(11):4142–54.
[52] Hodrokoukes P, Floudas G, Pispas S, Hadjichristidis N. Macromolecules 2001;34(3):650–7.
[53] Rubinstein M, Obukhov SP. Macromolecules 1993;26(7):1740–50.